A New Joint Tracking Method of BeiDou B1C Signal and Its Influence on Signal Quality Evaluation

Zhenyuan Hao[1,2], Chengyan He[1(✉)], Ji Guo[1,3], Xiaochun Lu[1,3], Yongnan Rao[1], and Meng Wang[1,2]

[1] National Time Service Center, Chinese Academy of Science, Xi'an 710600, China
hechengyan@ntsc.ac.cn
[2] School of Electronics, Chinese Academy of Science University, Beijing 101408, China
[3] School of Astronomy and Space Science, University of Chinese Academy of Sciences, Beijing 100098, China

Abstract. Aiming at the problem of low accuracy of traditional open-loop tracking and long time-consuming of closed-loop tracking, this paper proposes a joint open-loop and closed-loop tracking method of BeiDou B1C signal, which not only ensures the tracking accuracy but also greatly reduces the time-consuming of signal tracking. To verify the effectiveness and feasibility of the proposed algorithm, this paper uses the 40-m large aperture antenna system of Haoping observation station to collect the measured satellite signal data for verification and makes in-depth analysis from tracking time-consuming, correlation peak, correlation loss, zero-crossing deviation of S-curve, code and carrier phase consistency, etc. The results show that under the condition of the same tracking parameters when the data length ratio of the open-loop and the closed-loop parts is 9:1, the time of the method is saved about 90% compared with the closed-loop tracking method; at the same time, the difference of the three evaluation parameters is within 1%, which verifies the effectiveness and feasibility of the proposed method. The research results can provide a theoretical basis and technical support for parallel processing of navigation signals and automatic quasi-real-time signal quality monitoring and evaluation in the future.

Keywords: Open-closed-loop joint tracking · Closed-loop tracking · BeiDou B1C navigation signal · Signal quality evaluation

1 Introduction

As the link between satellite and user, the performance of the satellite navigation signal directly determines the service performance of the satellite navigation system, such as positioning, navigation, timing, and so on. Navigation signal quality monitoring and evaluation can provide important technical means and support for navigation system signal design and key technology on-orbit verification, and provide decision support

Q. Wu et al. (Eds.): WiSATS 2020, LNICST 357, pp. 449–467, 2021.
https://doi.org/10.1007/978-3-030-69069-4_37

information for system performance maintenance and management. It is an important means to ensure the safety, integrity, stability, and reliability of the satellite navigation system. Therefore, the monitoring and evaluation of navigation signal quality are one of the important links in the design and operation of the satellite navigation system.

To realize the interoperability with GPS L1C and Galileo E1: OS signals, the BeiDou B1C signal adopts Quadrature Multiplexed Binary Offset Carrier(QMBOC) modulation, the power spectral density, and autocorrelation function of QMBOC signal are the same as that of TMBOC signal, compared with the Time-Multiplexed Binary Offset Carrier(TMBOC) modulation signal, the receiver of QMBOC eliminates the switching circuit of time-division multiplexing locally, and they have the same performance under the condition of matching reception;

The design of Composite Binary Offset Carrier (CBOC) modulation signal determines that the power of its pilot component and data component is equal, while the power ratio of QMBOC signal components among different channels can be different, only the total power can meet the definition of normalized power spectral density of Multiplexing Binary Offset Carrier(MBOC) modulation signal, and its implementation mode is more flexible.

Before demodulating and fine analysis of satellite navigation signals, it is necessary to capture and track the signals. The tracking accuracy and time consuming directly affect the subsequent analysis and processing accuracy and data processing efficiency. Conventional closed-loop tracking takes the signal master code period as the loop phase and frequency identification period, and periodically adjusts the frequency and phase of carrier and code. Due to the loop input and output of data in each cycle, this method has high tracking accuracy, but the huge amount of computation and long-time consumption are not conducive to quasi-real-time signal analysis. The traditional open-loop tracking is based on the code phase shift and Doppler frequency shift obtained in the acquisition phase. The frequency and phase of carrier and code are directly used in the signal tracking phase through the least square estimation, Kalman filter, and other methods fitting. The computation is small and the time is short, but the error of various fitting models leads to poor tracking accuracy. In literature [1], the least square method and Kalman filtering method were used to optimize the estimation of the carrier frequency and the rough value of the code phase, which improved the estimation accuracy to a certain extent, but still could not achieve good stable tracking of the measured data. A JOINT GPS/Galileo tracking method based on maximum likelihood estimation was proposed in the literature [2]. Kalman filter is used to reduce noise and improve loop stability by using the error of code phase and frequency estimation generated by MLE, but the actual performance is not analyzed. Literature analyzes closed-loop serial processing and open-loop parallel processing [3] and verifies by combining INS and GPS deep combination system. Compared with the closed-loop system, the accuracy is not improved, but the complexity of the algorithm is increased. Literature adopts the methods of open-loop capture and closed-loop tracking to ensure tracking accuracy [4], but it takes a long time. To make up for these shortcomings, a new BeiDou open-closed-loop joint tracking method for the B1C signal is proposed. This method not only has good tracking accuracy but also can greatly improve the computing efficiency.

2 BeiDou B1C Signal Characteristics

The B1C signal is no longer a single signal, but a composite signal containing data and pilot channels. Among them, the data channel modulation has navigation message data, which can be used for pseudo-range measurement and navigation information solution, while the pilot channel does not modulate navigation information, but is only composed of spread spectrum code modulated by the carrier. In this way, the design can increase the coherence integration time at the receiving end and be used for pseudo-range measurement with higher accuracy [5]. B1C signal has higher tracking accuracy and anti-multi-path, anti-interference ability.

The power ratio of the B1C data component S_d and the pilot component S_p signal is 1:3. The data component was modulated with BOC(1, 1), and the pilot channel was modulated with QMBOC(6, 1, 4/33) orthogonal multiplexing of the high-frequency component BOC(6, 1) and the low-frequency BOC(1, 1) [6]. B1C signal structure is shown in Table 1 below:

Table 1. Signal structure of B1C

Component	Modulation		Phase relationship	Power ratio
$s_{B1C\_data}(t)$	Sine BOC (1, 1)		0	1/4
$s_{B1C\_pilot\_a}(t)$	QMBOC (6, 1, 4/33)	Sine BOC (1, 1)	90	29/44
$s_{B1C\_pilot\_b}(t)$		Sine BOC (6, 1)	0	1/11

B1C signal baseband form can be expressed as:

$$S_{B1C}(t) = \frac{1}{2}S_d + j\frac{\sqrt{3}}{2}S_p = \frac{1}{2}D_d \times C_d \times sign\left(\sin\left(2\pi f_{S\_d}t\right)\right) + \sqrt{\frac{1}{11}}C_p \times sign\left(\sin\left(2\pi f_{S\_b}t\right)\right) + j\sqrt{\frac{29}{44}}C_p \times sign\left(\sin\left(2\pi f_{S\_a}t\right)\right) \quad (1)$$

Where $D(t)$ is the navigation data stream, $C_d(t)$ is the data component spread spectrum code, $C_p(t)$ is the pilot component spread spectrum code, fS_a is the subcarrier frequency of narrow-band S_{pa}, and fS_b is the subcarrier frequency of narrow-band S_{pb}. $sign(\cdot)$ is a sign function.

3 Software Receiver Tracking Method

3.1 Principle of Open-Loop Tracking

The principle of open-loop tracking is shown in Fig. 1. $s_{IF}(n)$ is the input digital intermediate frequency signal, τ is the code phase offset of the input signal, f is the Doppler

frequency offset of the input signal, φ is the estimated carrier phase error value, i is the resulting signal of I-branch mixing, i_p is the correlation result, I_p is the coherent integral value, and f_{clock} is the driving clock frequency.

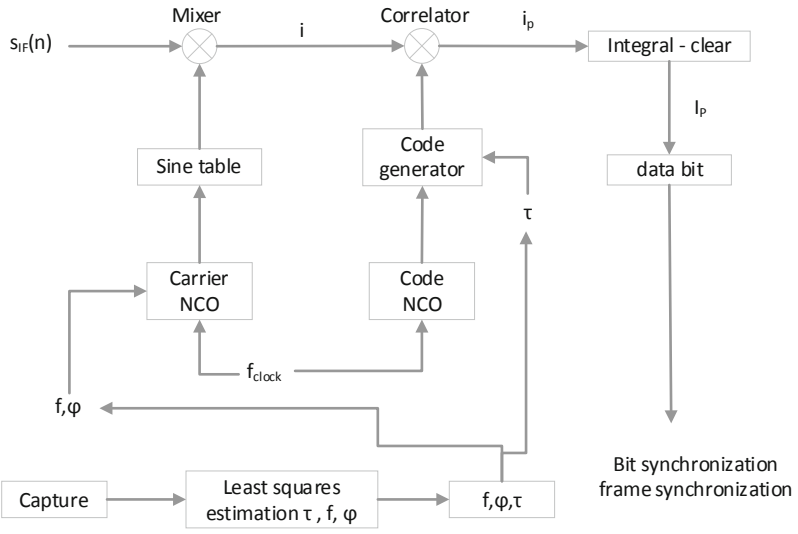

Fig. 1. Schematic diagram of open-loop tracking

The input signal is acquired by traditional acquisition to obtain rough Doppler frequency and code phase estimation value. Then, the least square criterion is used to fit the quadratic polynomial, and the peak value of the fitting curve is selected as the correction value of the Doppler frequency and code phase. The modified Doppler frequency, code phase, and carrier phase are output to the subsequent bit synchronization, frame synchronization, and other processing modules as the result of open-loop tracking [7].

The amplitude of the complex coherent integral value is:

$$V(\tau_e, f_e) = aR(\tau_e)|\sin c(f_e T_{coh})| + \varepsilon_n \tag{2}$$

Where, T_{coh} is coherent integration time, τ_e and f_e are doppler frequency and code phase estimation errors respectively, $R(\cdot)$ is code autocorrelation function, and $\sin c(\cdot)$ is energy fading function caused by Doppler frequency error. For the estimation of the Doppler frequency shift. It can be seen from the formula of complex coherent integral value that the profile of coherent integral value at any code phase is the result of function superposition noise, so the quadratic polynomial of linear least square fitting is used for parameter fitting.

3.2 Closed-Loop Tracking Principle

After the satellite signal is captured, the rough estimates of carrier frequency and code phase of the current satellite signal are obtained. However, due to the change of Doppler

effect caused by the relative motion between satellite and receiver and the change of relative acceleration, as well as the frequency offset between satellite clock and receiver clock crystal oscillator, the carrier frequency and code phase of the received satellite signal will change unpredictably with time. Therefore, it is necessary to process the satellite signal in the loop, that is, code tracking and carrier tracking. The specific tracking principle is shown in Fig. 2.

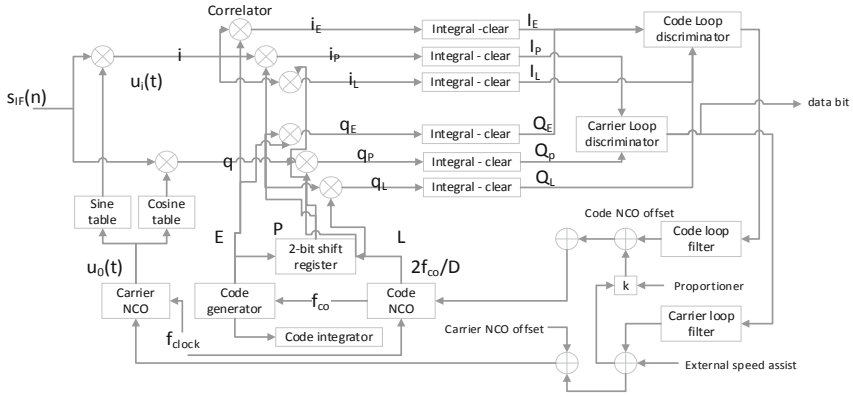

Fig. 2. Schematic diagram of closed-loop tracking

Carrier loop and code loop work simultaneously and coordinate with each other. Carrier loops with higher accuracy will carry out carrier assistance to the code loops at the frequency discrimination result, to eliminate the dynamic stress on the code loops and realize better loop tracking [8]. carrier loop is generally composed of a discriminator, loop filter, and Numerical Control Oscillator (NCO). THE Digital IF signal s_{IF} at I, Q is multiplied by sine and cosine respectively on the two branches, mixed with the local duplicated carrier signal (multiplied) to realize carrier separation, then the output signal is sent to the carrier loop discriminator for frequency identification, then it enters the filter to filter, finally, the output result is sent to the carrier NCO to calculate the phase difference, to adjust the local duplicated carrier signal and connect the local duplicated signal The phase difference between the received signals is always 0 to keep the continuous tracking of the signals. In the navigation receiver, Costas phase-locked loop is generally used, which is not sensitive to modulation data.

In the stage of carrier loop and code loop processing, the data of one main code cycle length is read each time for data analysis, and finally, the carrier phase difference is obtained to adjust the local recurrence signal of each loop and the received signal phase time to be consistent. The advantage of closed-loop in tracking is that the data of each main code cycle length is frequently discriminated against to ensure a high tracking accuracy.

3.3 Open-Closed-Loop Joint Tracking Mode

At present, the commonly used software and hardware receivers for satellite navigation signal processing are all based on the closed-loop tracking mode, which has the advantage

of being able to achieve high-precision and stable tracking of signals. However, the loop calculation is large and time-consuming, which is not conducive to quasi-real-time data analysis. Compared with the traditional closed-loop tracking method, the biggest difference of open-loop tracking is that the τ, f and φ obtained from the least square estimation are directly used for the tracking of subsequent data, rather than the feedback of the code phase and Doppler frequency output value to the tracking loop for frequency discrimination correction and output [9, 10]. The biggest advantage of open-loop tracking is that it saves a lot of time and cost, but the most fatal disadvantage is that it can't achieve accurate and stable tracking for the measured signal [11].

To ensure the tracking accuracy and improve the operational efficiency to the greatest extent, this paper proposes an open-closed-loop joint tracking method based on the advantages of open-loop tracking and closed-loop tracking. For the convenience of explanation, hereinafter referred to as joint tracking, the tracking principle is shown in Fig. 3.

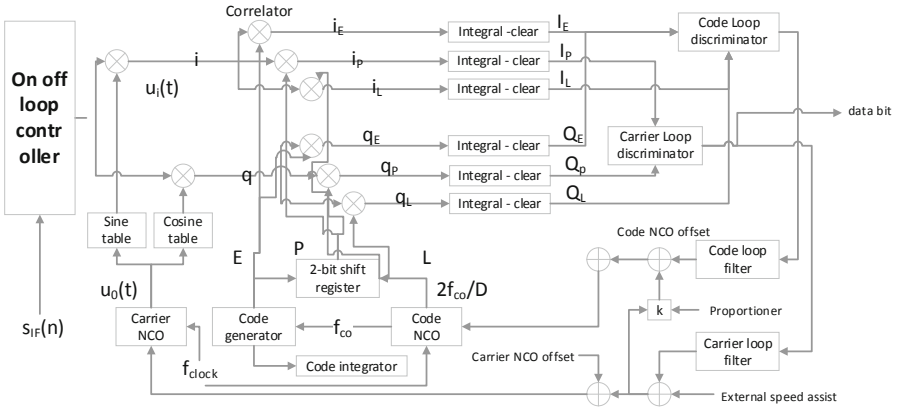

Fig. 3. Schematic diagram of open-closed-loop joint tracking mode

Generally, since the difference of carrier phase and the adjustment parameters of the code loop are very small for the data of tens or hundreds of milliseconds after the signal enters the stable tracking stage, a loop controller can be added to the feedback loop of the code loop and the carrier loop to realize the joint tracking of open-loop and closed-loop tracking. Because the frequency discrimination times of carrier loop and code loop are reduced, the tracking time of the signal is greatly reduced.

The loop control principle is shown in Fig. 4. First, set the open-loop interval according to the signal characteristics and data quality, for example, 100 ms. The loop input signal $s_{IF}(n)$ first judges the tracking mode adopted by the data of the period length of the main code through the loop controller. If the open-loop tracking is adopted, the loop output parameters of the previous closed-loop tracking will be assigned to the current open-loop tracking. If the closed-loop tracking is adopted, the normal tracking will be conducted according to the flow shown in Fig. 2, and finally a complete loop will be formed. The main function of the closed-loop tracking is to adjust the phase and frequency of the locally repeated carrier and code through the periodic output of the loop,

so that it is strictly consistent with the frequency and phase of the input signal, to achieve a high-precision tracking effect.

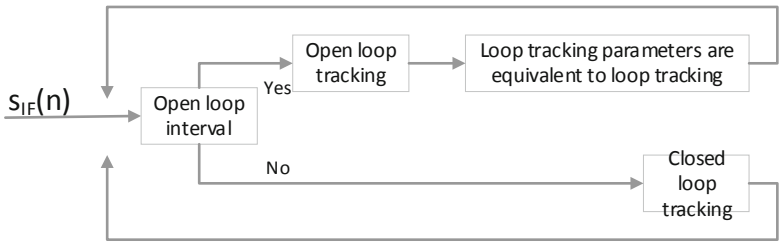

Fig. 4. Schematic diagram of the loop controller

The input and output signals of the loop are expressed as follows:

$$u_i(t) = U_i \sin(\omega_i t + \theta_i) \tag{3}$$

$$u_0(t) = U_0 \sin(\omega_0 t + \theta_0) \tag{4}$$

$u_i(t)$ and $u_0(t)$ represent the input and output signals of the loop discriminator respectively, and U_i,U_0 represent the signal amplitude of the input and output signals of the loop discriminator respectively. The angular frequency ω_i and the initial phase θ_i of the input signal and the angular frequency ω_0 and the initial phase θ_0 of the output signal are both functions of time.

The open-loop tracking and closed-loop tracking are organically combined by the open-closed-loop controller. The closed-loop tracking part ensures the tracking accuracy, and the open-loop tracking part reduces the tracking time. The advantages of the two are combined by the open-closed-loop controller.

4 Main Parameters of Signal Quality Evaluation

4.1 Correlation Peak

The distortion of the received navigation satellite signal chip waveform is not only reflected in the amplitude attenuation of the correlation output but also causes the deformation of the correlation function [12]. The pseudo-range error caused by the distortion of the received signal can directly reflect the abnormality of the correlation function. Using the correlation curve, we can evaluate the correlation power loss caused by channel band limit and distortion and its influence on navigation performance. Firstly, according to the output of the tracking loop of the software receiver, carrier stripping, and Doppler removal are carried out for the received navigation satellite signal, and the measured signal ranging code is obtained by equalizing the measured channel transmission characteristics. The normalized cross-correlation between the measured signal and the local

reference code is calculated. The definition is as follows:

$$CCF(\tau) = \frac{\int_0^{Tp} S_{BB-PreProc}(t) \cdot S^*_{Ref}(t-\tau)dt}{\sqrt{\left(\int_0^{Tp} |S_{BB-PreProc}(t)|^2 dt\right) \cdot \left(\int_0^{Tp} |S_{Ref}(t)|^2 dt\right)}} \tag{5}$$

Where: $S_{BB-PreProc}(t)$ is the ranging code of the measured satellite signal; S_{Ref} is the ideal replication code generated by the local receiver; the integration time T_p usually corresponds to a main code period of the reference signal.

In the practical system engineering, to get the correlation function of higher time-domain resolution, the sampling rate of the digital signal should be increased, or multi-period overlapping accumulation technology should be used. To reduce the influence of noise, the correlation function can be averaged in multiple code periods.

4.2 Correlation Loss

Correlation loss refers to the difference between the received signal power in the designed frequency band bandwidth and the recovered signal power in the ideal correlation receiver in the same frequency band bandwidth. In the ideal correlation receiver, the input is the ideal signal waveform, the filter is the bandwidth designed for the signal, and the inner phase of the bandwidth is the linear ideal sharp cut-off filter.

The correlation loss is calculated as follows:

$$P_{CCF}[dB] = \max_{\substack{aver \\ all}} \left(20 \cdot \log_{10}(|CCF(\varepsilon)|)\right) \tag{6}$$

$$CL_{\text{Distortion}}[dB] = P_{\substack{CCF \\ IdealS_{Input}}}[dB] - P_{\substack{\text{CCF} \\ \text{Real}S_{Input}}}[dB] \tag{7}$$

Where P_{CCF} represents signal power, $P_{\substack{CCF \\ IdealS_{Input}}}$ represents ideal signal power, $P_{\substack{\text{CCF} \\ \text{Real}S_{Input}}}$ represents received signal power, and $CL_{\text{Distortion}}$ represents correlation loss.

The lower the correlation loss, the higher the pseudo-range measurement accuracy, and the lower the receiver threshold [13]. When using the above formula to calculate the correlation loss, we should also consider the influence of the relative change of power distribution between different bandwidth signal components caused by the actual band-limited filter on the calculation results.

4.3 Zero Crossing Deviation of S-Curve

Theoretically, the Zero crossing point of the receiver code loop frequency discrimination curve (S-curve), that is, the lock point of the code loop, should be located at the point where the code tracking error is zero. In fact, due to the influence of channel transmission distortion and multipath, the frequency discrimination curve of the code loop is often locked in the place with phase deviation [14].

Taking the noncoherent lead-lag power frequency discriminator as an example, if the lead-lag distance of the correlator is δ, the S-curve can be expressed as follows:

$$SCurve(\varepsilon, \delta) = \left|CCF\left(\varepsilon - \frac{\delta}{2}\right)\right|^2 - \left|CCF\left(\varepsilon + \frac{\delta}{2}\right)\right|^2 \tag{8}$$

The deviation of the locking point $\varepsilon_{\text{bias}}(\delta)$ satisfies:

$$SCurve(\varepsilon_{\text{bias}}(\delta), \delta) = 0 \tag{9}$$

In particular, when there is more than one zero-crossing (such as BOC modulation signal), the zero-crossing nearest to the maximum correlation power shall be selected.

S-curve deviation is defined as:

$$SCB = \max_{\substack{over \\ all\delta}}(\varepsilon_{\text{bias}}(\delta)) - \min_{\substack{over \\ all\delta}}(\varepsilon_{\text{bias}}(\delta)) \tag{10}$$

The value range δ is $[0, \delta_{\max}]$ and the value of $\delta_{\max}$ is as follows:

$$\delta_{\max}[\text{chips}] = \begin{cases} \frac{1.5}{4\frac{m}{n}-1} & BOC(m,n) \text{ signal} \\ 1.5 & BPSK-n \text{ signal} \end{cases} \tag{11}$$

From the expression of S-curve and the deviation of the locking point $\varepsilon_{\text{bias}}(\delta)$, we can draw the curve of the deviation of the locking point $\varepsilon_{\text{bias}}(\delta)$ with the distance δ. Besides, to minimize the impact of noise, average processing can be performed in multiple code cycles. At the same time, to reduce the influence of cross-correlation between different signal components, it is necessary to average for different cross-correlation situations. In the calculation process, the influence of uncertainty and instability introduced by the measurement system itself should be avoided as far as possible.

4.4 Code and Carrier Phase Consistency

By evaluating the consistency of ranging code pseudo-range and carrier phase pseudo-range, the relative jitter between code and carrier in the modulation process of the satellite navigation signal is measured. Because the output value of the carrier phase observation of the receiver is not the absolute carrier phase output, but relative to the relative carrier phase output at a certain time, at present, the consistency evaluation is mainly to evaluate the relative stability of the code and the carrier phase.

$$\begin{aligned} \Delta\rho_N &= \rho_{N+1} - \rho_N \\ \Delta\Phi_N &= \Phi_{N+1} - \Phi_N \\ \Phi_N &= \psi_N \times C/\left(f_0 + f_{Ndpp}\right) \\ \Delta &= \Delta\rho_N - \Delta\Phi_N \end{aligned} \tag{12}$$

The ρ_N and ψ_N represents the code pseudo distance and the carrier phase output of the receiver, c represents the speed of light, the value is 299792458 m/s, f_0 represents the signal center frequency, f_{Ndpp} represents the Doppler frequency shift, and Δ represents the pseudo-range difference between the code and the carrier phase in units of distance.

5 Open-Closed-Loop Tracking Test Results

Using the 40-mlarge aperture antenna system at Haoping observation station in Luonan, Shaanxi Province, to observe and collect the satellite downlink signal data, taking the

BeiDou Global System MEO-2 satellite as an example, the acquisition card parameters are set with the sampling rate of 250 MHz, the acquisition time of 3 s, and the data of 2–3 s that the signal enters the stable tracking are taken for the comparison and signal quality evaluation of the two tracking methods (1) the closed-loop tracking parameters are set with the carrier loop bandwidth 20 Hz, damping factor $\sqrt{2}/2$, code loop bandwidth 5 Hz, damping factor $\sqrt{2}/2$, correlator interval 0.1, loop cycle 10 ms; (2) the joint tracking parameters are consistent with the closed-loop, and the loop cycle of three components B1Cd, B1Cpa and B1Cpb is 100 ms.

In the following, the time-consuming and the impact of signal quality evaluation results are compared and analyzed in depth.

5.1 Time-Consuming Comparison

The loop period of 10 ms is adopted for the closed-loop tracking of the BeiDou B1C signal, and 100 ms is adopted for the joint tracking. The two concentric rings represent the output of the loop result, the phase discrimination of the loop, and the time-consuming proportion of the filtering from the outside to the inside; the first and second sectors represent the joint tracking and the closed-loop tracking respectively from 0 degrees clockwise. The time-consuming statistics are as follows:

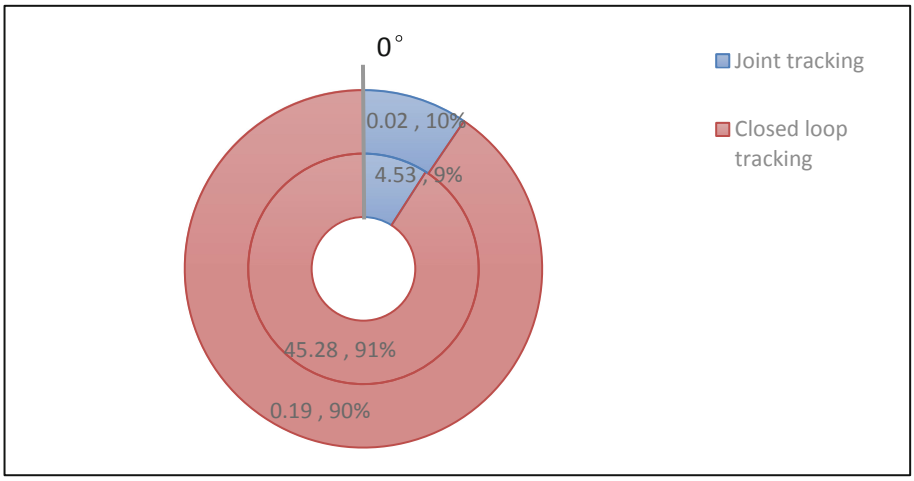

Fig. 5. Open closed-loop tracking time chart (time/s)

The actual data analysis results show that:

The signal tracking process is mainly composed of carrier and pseudo code separation, loop phase discrimination, and filtering, and the time ratio of joint tracking and closed-loop tracking is about 1:10. The separation process of carrier and pseudo code is the most computationally intensive and takes up the most time. The total time of joint tracking is 4.554 s, and the total time of closed-loop tracking is 45.535 s, which saves about 90% of the time compared with closed-loop tracking.

5.2 Comparison of Signal Evaluation Results

Comparison of Tracking Results

Figure 6, 7 and 8 shows the tracking results of three signal components of B1C. The dotted line represents closed-loop tracking and the solid line represents joint tracking. Compared with the closed-loop tracking, the overall trend of the output value of the loop discriminator and the output value of the loop filter in the open-closed-loop tracking method is basically consistent with that of the traditional closed-loop tracking method, which shows that this method can realize the stable tracking of the signal.

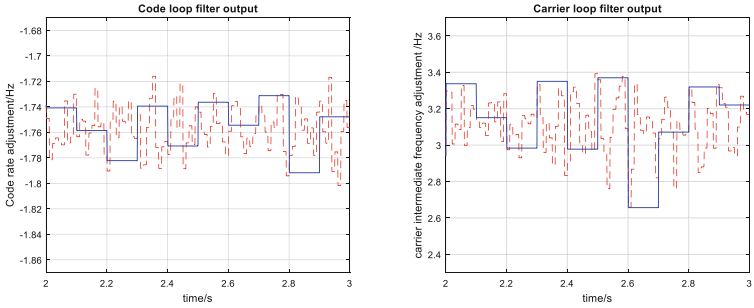

Fig. 6. B1Cd tracking results

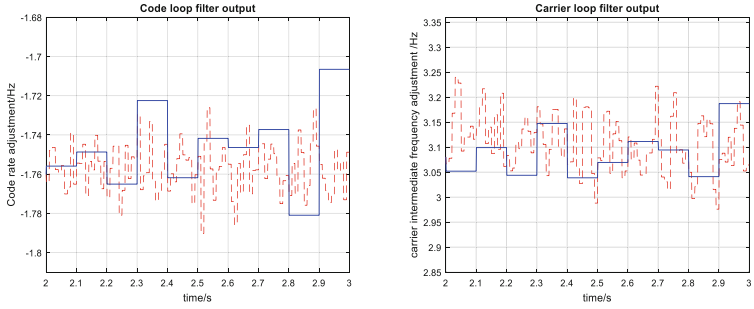

Fig. 7. B1Cpa tracking results

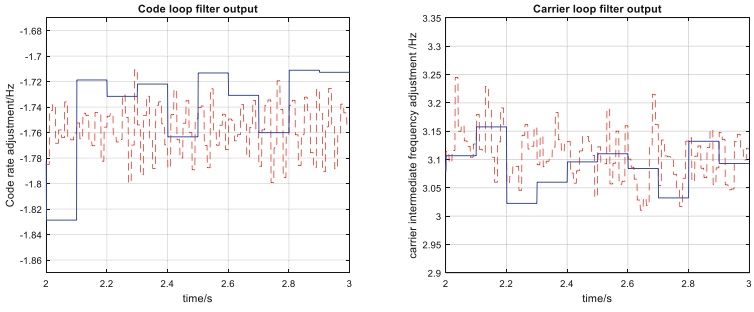

Fig. 8. B1Cpb tracking results

Comparison of Signal Quality Evaluation Results

Correlation Curve

Figure 9, 10 and 11 shows the correlation curve of three signal components of B1C calculated by Eq. (5). In these figures, the solid line represents the ideal signal, the dotted line represents the closed-loop tracking signal, and the triangle solid line represents the joint tracking signal. The right figure is the amplification diagram at the correlation peak.

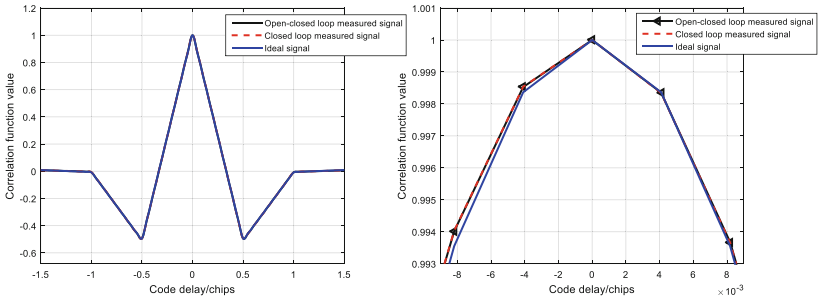

Fig. 9. B1Cd correlation curve

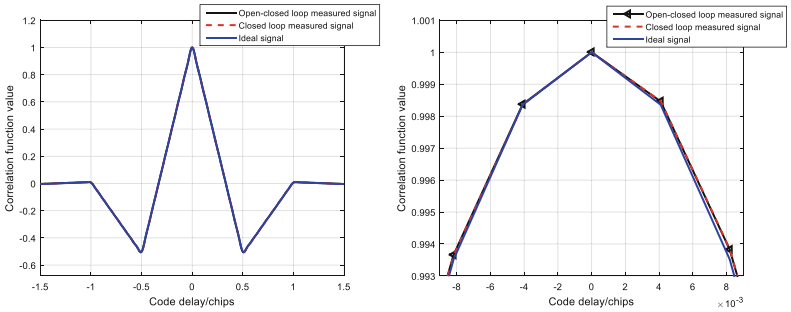

Fig. 10. B1Cpa correlation curve

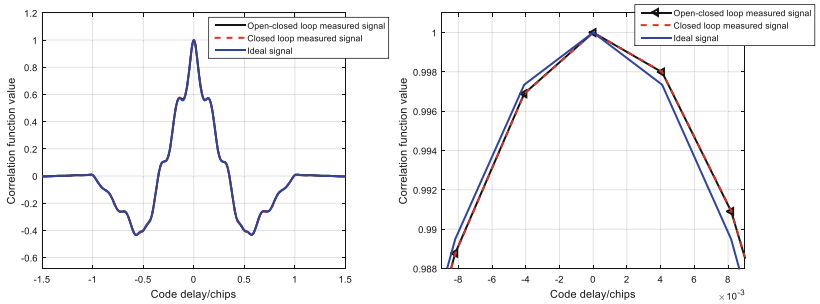

Fig. 11. B1Cp correlation curve

To analyze and compare the symmetry, smoothness, and coincidence degree of the curves, the whole correlation curve is moved to 0 chip.

From the comparison of Fig. 9, 10 and 11, it can be seen that the joint tracking method basically coincides with the correlation curve of the traditional closed-loop tracking.

Table 2 shows the mean value and standard deviation of the correlation curve difference between the two tracking methods of each component.

Table 2. Correlation curve differences

Signal component	Mean value	Standard deviation
B1Cd	−2.8002e−07	5.4571e−06
B1Cpa	−1.4064e−07	1.3141e−05
B1Cp	−1.0715e−07	1.1267e−05

According to Table 2, the difference between the two tracking methods of each component is very small, and the curve coincidence is high.

Correlation Loss

Figure 12, 13 and 14 shows the correlation loss figure of each component calculated once every 50 ms in two tracking methods, with a total of 20 times. The horizontal line with a value of 0.3 represents the evaluation index. Take the mean value and get the correlation loss evaluation results in Table 3 through correlation calculation.

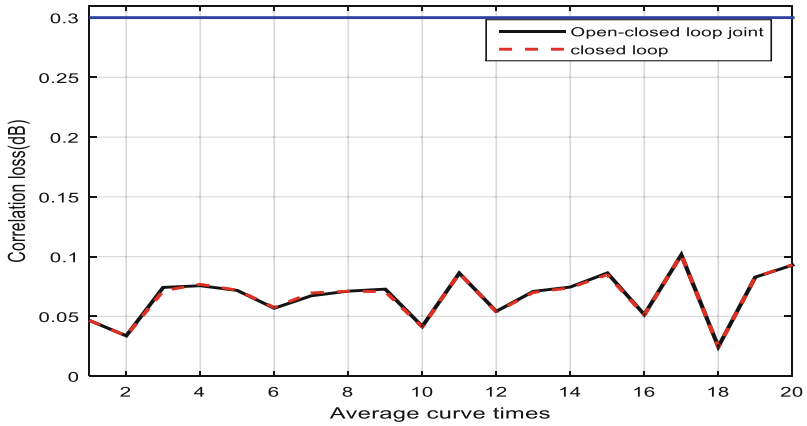

Fig. 12. B1Cd correlation loss

It can be seen from Fig. 12, 13 and 14 that the correlation loss of the three signal components is less than the index requirement of 0.3 dB in the BeiDou ICD document and the variation degree of each correlation loss value is small.

Table 3 shows the mean value and standard deviation of the correlation loss difference of each component in two tracking methods.

From Table 3, it can be seen that the difference between the two tracking methods of each component is very small, and the curve coincidence is high.

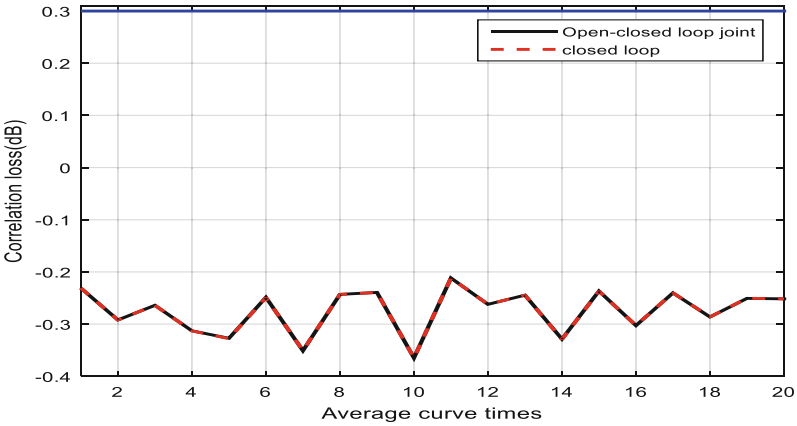

Fig. 13. B1Cpa correlation loss

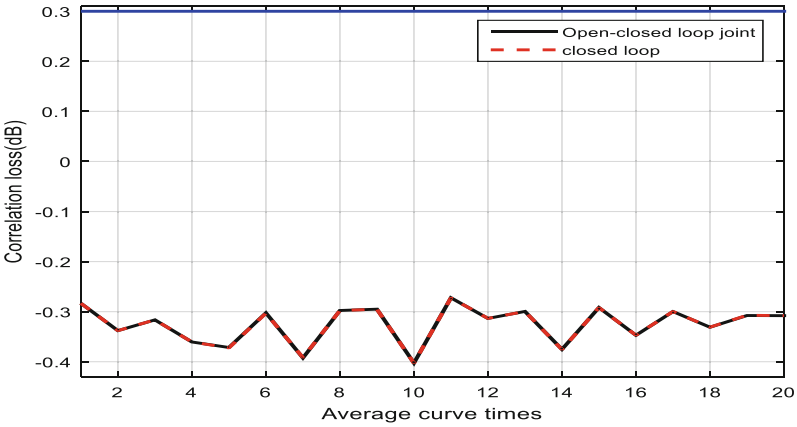

Fig. 14. B1Cp correlation loss

Table 3. Correlation loss difference (dB)

Signal component	Mean value	Standard deviation
B1Cd	2.3949e−04	3.1941e−04
B1Cpa	7.5931e−05	2.6769e−04
B1Cp	4.5124e−05	3.0863e−04

Table 4 shows the correlation loss values corresponding to the two tracking methods of each component, and the index requirements are not more than 0.3 dB

Table 4. Correlation loss (dB)

Signal component	Index	Closed-loop	Joint tracking
B1Cd	≤0.3	0.066587	0.066827
B1Cpa		−0.274641	−0.274566
B1Cp		−0.325460	−0.325415

From Table 4, it can be seen that the variation range of the correlation loss value of joint tracking is within 0.4% compared with that of closed-loop tracking, and the difference between the two is very small.

Zero Crossing Deviation of S-curve

Figure 15, 16, 17 and 18 shows the Zero crossing deviation of the S-curve of each component in two tracking modes. The difference between the maximum value and the minimum value of the curve in these figures is the Zero crossing deviation of the curve in Table 5. B1cp 0.16–0.36 chip peak skew summit results in a large range deviation, which will be abandoned as an evaluation index. Figure 17 shows the SCB value at b1cp 0.01–0.15 chip and Fig. 18 shows the SCB value at b1cp 0.37–0.46 chip.

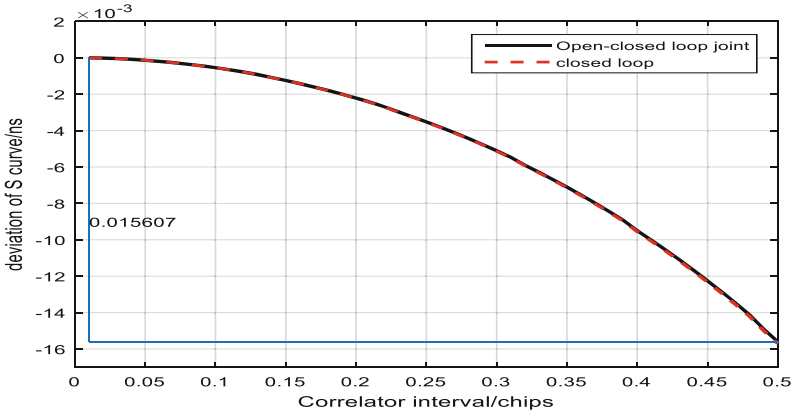

Fig. 15. B1Cd SCB

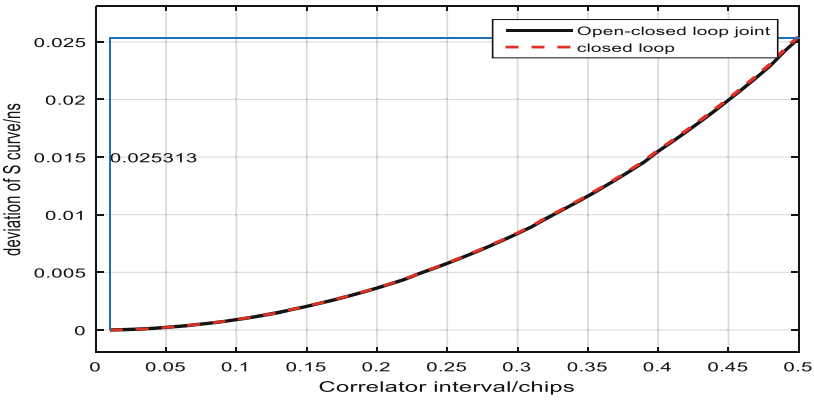

Fig. 16. B1Cpa SCB

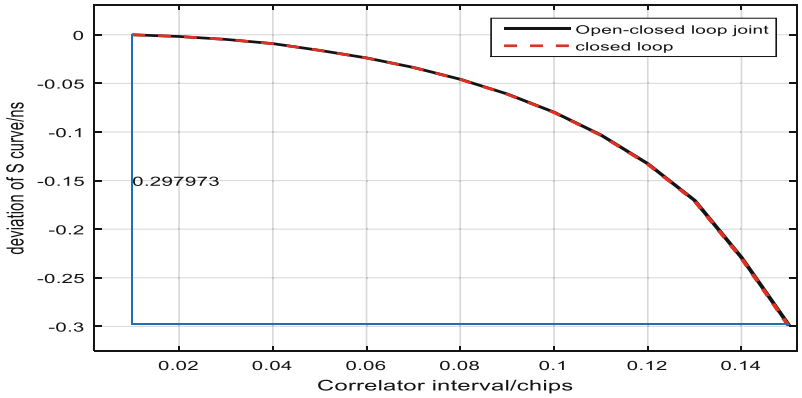

Fig. 17. B1Cp (0.15chip) SCB

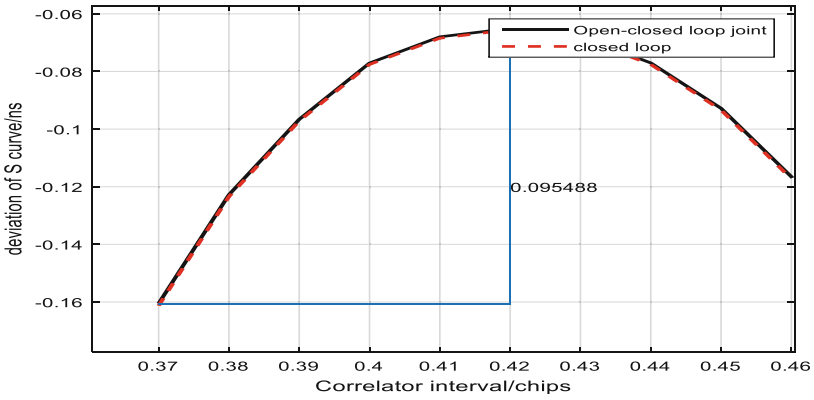

Fig. 18. B1Cp(0.46chip) SCB

Table 5. S zero-crossing deviation difference of curve (ns)

Signal component	Mean value	Standard deviation
B1Cd	2.8776e−05	2.9175e−05
B1Cpa	−5.4799e−05	5.1520e−05
B1Cp (0.15chip)	2.8763e−04	3.2261e−04
B1Cp (0.46chip)	7.8407e−04	3.9641e−04

It can be seen from Fig. 15, 16, 17 and 18 that the SCB curves of the two tracking modes of each component are coincident.

Table 5 shows the mean value and standard deviation of the zero-crossing deviation of the S-curve of each component in two tracking methods.

It can be seen from Table 5 that the difference between the two tracking methods of each component is very small and the curve coincidence is high.

Table 6 shows the zero-crossing deviation value of S-curve corresponding to the two tracking methods of each component and meets the index requirements of no more than 0.5 ns.

Table 6. Zero-crossing deviation of S-curve (ns)

Signal component	Index	Closed-loop	Joint tracking
B1Cd	≤0.5	0.015707	0.015607
B1Cpa		0.025482	0.025313
B1Cp (0.15chip)		0.299040	0.297973
B1Cp (0.46chip)		0.095802	0.095488

From Table 6, it can be seen that the value range of SCB of each component of joint tracking is within 0.7% compared with that of closed-loop tracking, and the difference between them is very small.

Code and Carrier Phase Consistency

Table 7 shows the average consistency of code and carrier phase corresponding to the two tracking methods of each component and meets the requirement of no greater than the index 1°.

It can be obtained from Table 7 that there is basically no difference in the result of phase consistency between each component code and carrier phase of joint tracking compared with closed-loop tracking.

Table 7. Consistency average of code and carrier phase (°)

Signal component	Index	Closed-loop	Joint tracking
B1Cd	≤1	−0.024899	0.025039
B1Cpa		−0.075774	−0.077376
B1Cp		−0.230170	−0.307586

6 Conclusion

This paper first introduces the principle and characteristics of traditional open-loop tracking and traditional closed-loop tracking. Because the traditional open-loop tracking takes less time and the traditional closed-loop tracking method has high tracking accuracy, this paper makes full use of the advantages of the open-loop tracking and the closed-loop tracking, proposes a new open-closed-loop joint tracking method for the BeiDou B1C signal, and makes use of the BeiDou total collected by Haoping observation station The validity and feasibility of the proposed method are verified by analyzing the measured data of the downlink signal of MEO-2 satellite. Taking the data of 2–3 s that the signal enters into the stable tracking to compare the two tracking methods and evaluate the signal quality, the research results show that:

1. Under the condition of the same measured signal and the same receiver tracking parameters, the data length ratio of open-closed-loop tracking of Joint tracking is 1:9, and the tracking time of the open-closed-loop joint tracking method is about 90% less than the traditional closed-loop tracking method.
2. The mean and standard deviation of the difference between the two correlation curves are very small, and the degree of curve coincidence and the symmetry of the left and right overall are relatively high.
3. The change range of correlation loss values of the two tracking methods is within 0.4%, the difference between them is very small, and both are less than the 0.3 dB index requirements in the BeiDou ICD document.
4. The coincidence degree of SCB curves of the two tracking methods is very high, and the value range of SCB is within 0.7%, which meets the index requirements of 0.5 ns.
5. There is basically no difference between the code and carrier phase consistency mean results of the two tracking methods.

Therefore, the open-closed-loop joint tracking method proposed in this paper can greatly improve the efficiency of data processing based on ensuring the tracking effect.

The next step is to further study the method of intelligent control and adjustment of loop controller parameters by a loop feedback mechanism, and analyze whether the joint tracking sensitivity of different signal components to the same time is the same.

References

1. Lv, F.: Open-loop tracking design and performance analysis of the satellite navigation receiver. Beihang University (2015)
2. Won, J., Pany, T., Eissfeller, B.: Design of a Unified MLE tracking for GPS/Galileo software receivers (2006)
3. Van, G.F., Soloviev, A., Uijt, D.H.M., et al.: Closed-loop sequential signal processing and open-loop batch processing approaches for GNSS receiver design. IEEE J. Select. Top. Sig. Process. **3**(4), 571–586 (2009). https://doi.org/10.1109/jstsp.2009.2023350
4. Han, C., Bai, Y., Si, J.: Carrier synchronization algorithm of joint open-loop acquisition and closed-loop tracking in a highly dynamic environment. J. Northwest. Polytech. Univ. **36**(06), 1232–1235 (2018)
5. Guo, Y.: Research on high precision tracking and evaluation technology of the BeiDou B1C signal. UCAS(NTSC) (2019)
6. Academic exchange center of China Satellite Navigation System Management Office.: BeiDou Navigation Satellite System Signal In: Space Interface Control Document Open Service Signal B1C (Version 1.0). Beijing: China Satellite Navigation System Management Office (2017)
7. Li, Z., Zhang, T., Yan, K., et al.: A phase prediction method for improving carrier phase continuity of GPS receiver. J. Geodesy Geodyn. **38**(12), 1280–1284 (2018). https://doi.org/10.14075/j.jgg.2018.12.013
8. Feng, Z.: Study on LEO-LEO occultation signal receiving technology. UCAS(NTSC) (2018)
9. Jing, S.: Research on performance evaluation and auxiliary enhancement technology of GNSS space service airspace. Shanghai Jiao Tong University (2017)
10. Han, S., Wang, W., Chen, X., et al.: High dynamic carrier tracking loop based on the UKF quasi-open loop structure. Acta Aeronaut. ET Astronaut. Sin. **31**(12), 2393–2399 (2010)
11. Yan, K.: Research on scalar deep combined baseband technology for GNSS high precision positioning in urban complex environment. WuHan University (2018)
12. He, C., Lu, X., Guo, J.: A new method to evaluate the waveform distortion of the satellite navigation signal. J. Electron. Inf. Technol. **41**(05), 1017–1024 (2019)
13. Hauschild, A., Montenbruck, O.: A study on the dependency of GNSS pseudorange biases on correlator spacing. GPS Solutions **20**(2), 159–171 (2014). https://doi.org/10.1007/s10291-014-0426-0
14. He, C., Lu, X., Guo, J., et al.: Initial analysis for characterizing and mitigating the pseudorange biases of the BeiDou navigation satellite system. Satell. Navig. **1**(11) (2020). https://doi.org/10.1186/s43020-019-0003-3